A vortex in an infinite viscous fluid

By ROBERT R. LONG
Department of Mechanics, The Johns Hopkins University

(Received 23 June 1961)

A solution is given for a viscous vortex in an infinite liquid. Similarity arguments lead to a reduction of the equations of motion to a set of ordinary differential equations. These are integrated numerically. A uniform feature is the constant circulation K outside the vortex core, which is also a viscous boundary layer. The circulation decreases monotonically towards the axis. The axial velocity profiles and the radial velocity profiles have several characteristic shapes, depending on the value of the non-dimensional momentum transfer M. The solution has a singular point on the axis of the vortex. The radius of the core increases linearly with distance along the axis from the singularity, and, at a given distance, is proportional to the coefficient of viscosity and inversely proportional to K.

Finally, a discussion is given to indicate that intense vortices above a plate, like the confined experimental vortex, or above the ground, like the atmospheric tornado and dust whirl, will not resemble the theoretical vortex except, possibly, far above the plate.

1. Introduction

This paper extends an earlier investigation (Long 1958) of a vortex in an infinite viscous liquid. The earlier paper contained the general form of the solution together with the set of ordinary non-linear differential equations to which the Navier–Stokes equations reduce. These ordinary differential equations can be simplified by a boundary-layer approximation. The simplified equations have now been integrated numerically for a considerable range of the single governing parameter, and the numerical results are presented below.

This study was motivated by an experiment with a hydrodynamic 'sink' at the axis of a tall rotating cylinder of water (Long 1956). When the sink was very weak the fluid approached in an intense vortex along the axis of rotation (figure 1, plate 1). Observations of this vortex suggested the general form of the theory as developed in the first paper, in particular the boundary-layer nature of the core and the tendency for a 'vr-vortex' to arise outside the core.

Although it was originally thought that the theoretical and experimental vortices might be closely related, a recent comparison of the numerical and theoretical results showed that there are fundamental differences that arise, apparently, from the presence of the boundaries in the experiment. The fluid in the core of the vortex of figure 1 (plate 1) originates in the boundary layer on the lower plate, and the effect of friction, as this fluid moves over the relatively short distance from the lower plate to the sink, is doubtless too slight to produce the

kind of velocity profile found in the theory of this paper. The present theory should be applicable to a vortex above a plate, as in figure 1, but only at much greater distances from the plate than the metre or so that was available in this experimental set-up. This is discussed at greater length in §5 below.

2. Review of theory

We present here, briefly, the essential parts of the theory of the viscous vortex, including some of the work of the earlier paper (Long 1958). We assume the existence of a laminar vortex in an infinite viscous liquid centred at the axis of a cylindrical co-ordinate system (r, ϕ, z). The motion is axisymmetric, and the fluid has a constant density ρ and kinematic coefficient of viscosity ν. The equation of continuity implies a stream function $\psi(r, z)$ such that

$$u = -\frac{1}{r}\frac{\partial \psi}{\partial z}, \quad w = \frac{1}{r}\frac{\partial \psi}{\partial r}, \tag{1}$$

where

$$u = \frac{dr}{dt}, \quad w = \frac{dz}{dt}. \tag{2}$$

The third component of velocity is

$$v = r\frac{d\phi}{dt}. \tag{3}$$

We assume that the circulation vr tends to a constant K at great enough distances from the axis. Another fundamental constant of the problem is the kinematic momentum transfer

$$J = \int_0^{2\pi}\int_0^{\infty} (P + w^2)\, r\, dr\, d\phi, \tag{4}$$

where $P = p/\rho + gz$. We may show that the integral in (4) is constant by integrating the vertical component of the equations of motion over a plane perpendicular to the vortex axis and assuming that the velocities go to zero sufficiently fast at great distances from the axis.

If we suppose now that the conditions of the problem introduce no other parameters, then ψ, v and P are functions of r, z, J, K, ν only. A dimensional analysis leads to the form of the solution

$$\psi = \nu z f(y), \quad v = \frac{K}{r}\Gamma(y), \quad P = -\frac{K^4}{\nu^2 z^2}s(y), \tag{5}$$

$$w = \frac{K}{r\sqrt{2}}f', \quad u = -\frac{\nu}{r}f + \frac{K}{z\sqrt{2}}f', \quad y = \frac{Kr}{\nu z\sqrt{2}}, \tag{6}$$

where f, Γ, s are functions also of the inverse Reynolds number and non-dimensional momentum transfer

$$\epsilon = \frac{\nu}{K}, \quad M = \frac{J}{K^2}. \tag{7}$$

The assumed solution has a singularity at $z = 0$, $r = 0$. A prominent feature of the motion is that the circulation vr is constant on cones with apexes at the singular point.

Substituting into the equations of motion in cylindrical co-ordinates, we find that the functions f, Γ, s must satisfy the equations (Long 1958)

$$\Gamma^2 + 2y^3 s' = -\epsilon^2(f^2 - ff'y + y^2 f'' + 8y^4 s - yf' + 4y^5 s') - \epsilon^4(2y^4 f''), \tag{8}$$

$$f''y - f'(1-f) - 4y^3 s = -\epsilon^2(2f''y^3), \tag{9}$$

$$\Gamma''y - \Gamma'(1-f) = -\epsilon^2(2\Gamma''y^3 + 4\Gamma' y^2). \tag{10}$$

Obviously a boundary-layer approximation, $\epsilon^2 \ll 1$, is in order, and we will confine attention to such cases. Our equations are then

$$\Gamma^2 + 2y^3 s' = 0, \tag{11}$$

$$f''y - f'(1-f) - 4y^3 s = 0, \tag{12}$$

$$\Gamma''y - \Gamma'(1-f) = 0. \tag{13}$$

3. Numerical solution

Solutions of equations (11)–(13), subject to physical boundary conditions, were obtained numerically on an IBM 704 electronic computer. If we impose finiteness conditions at the axis $y = 0$, the solution of (11)–(13) near $y = 0$ is

$$f = ay^2 + a_4 y^4 + \ldots, \tag{14}$$

$$\Gamma = by^2 + b_4 y^4 + \ldots, \tag{15}$$

$$s = c + c_2 y^2 + \ldots, \tag{16}$$

where $$a_4 = \tfrac{1}{2}c - \tfrac{1}{4}a^2, \quad b_4 = -\tfrac{1}{4}ba, \quad c_2 = -\tfrac{1}{4}b^2, \quad \ldots,$$

and in general all coefficients are functions of a, b, c. On the other hand, the system (11)–(13) has an asymptotic solution at large y of the form

$$f = f_0 + \beta f_1 + \beta^2 f_2 + \ldots, \tag{17}$$

$$\Gamma = c_1 + \beta\Gamma_1 + \beta^2\Gamma_2 + \ldots, \tag{18}$$

$$s = c_2 + c_1^2/4y^2 + \beta s_1 + \beta^2 s_2 + \ldots. \tag{19}$$

Here, β, c_1 and c_2 are constants, and f_0 satisfies the differential equation

$$f_0''y - f_0'(1-f_0) - 4y^3 c_2 - c_1^2 y = 0.$$

The functions f_n, Γ_n, s_n all satisfy conditions of the form $f_n/f_{n-1} \to 0$ at large y. There is a total of five arbitrary constants in (17)–(19), so that it is reasonable to assume that solutions (for arbitrary choice of a, b, c, for example) have the behaviour

$$f \to f_0, \tag{20}$$

$$\Gamma \to c_1, \tag{21}$$

$$s \to c_2 + c_1^2/4y^2, \tag{22}$$

as $y \to \infty$. This assumption was the basis of the numerical integration.

Two conditions must be imposed as $y \to \infty$: (1) $c_2 = 0$, insuring uniform (zero) pressure far from the vortex axis; (2) $c_1 = 1$, insuring that the circulation tends to K. We see then that one of the constants a, b, c is arbitrary. Alternatively, the problem is determined by specifying the constant non-dimensional momentum transfer, M.

When $c_1 = 1$ and $c_2 = 0$, we may substitute $\Gamma_0 = 1$, $s_0 = 1/4y^2$ into (11)–(13) and obtain a single differential equation for f_0. This equation may be solved quite generally, and it is found that the solution tends to $1+y$, which is also a particular solution of the differential equation. With $f \to 1+y$, $\Gamma \to 1$, we can write down the behaviour at infinity of the velocity components:

$$u \to -\frac{\nu}{r}, \quad w \to \frac{K}{r\sqrt{2}}, \quad v \to \frac{K}{r}. \tag{23}$$

We may now proceed as follows. Define

$$x = c^{\frac{1}{4}}y, \quad A = -ac^{-\frac{1}{2}}, \quad B = bc^{-\frac{3}{4}}, \tag{24}$$

$$z_1 = c^{-\frac{1}{2}}\Gamma, \tag{25}$$

$$z_2 = c^{-1}s, \tag{26}$$

$$z_3 = -c^{-\frac{1}{4}}f/y, \tag{27}$$

$$z_4 = c^{-\frac{1}{2}}f'/y, \tag{28}$$

$$z_5 = c^{-\frac{3}{4}}\Gamma'/y. \tag{29}$$

The differential equations become

$$\dot{z}_1 = xz_5, \tag{30}$$

$$\dot{z}_2 = -z_1^2/2x^3, \tag{31}$$

$$\dot{z}_3 = -z_4 - z_3/x, \tag{32}$$

$$\dot{z}_4 = 4xz_2 + z_3z_4, \tag{33}$$

$$\dot{z}_5 = z_3z_5, \tag{34}$$

where the dot denotes differentiation with respect to x. The solutions near $x = 0$ are

$$z_1 = Bx^2 + B_4x^4 + \ldots, \tag{35}$$

$$z_2 = 1 + \gamma_2x^2 + \ldots, \tag{36}$$

$$z_3 = Ax + A_3x^3 + \ldots, \tag{37}$$

$$z_4 = -2A - 4A_3x^2 + \ldots, \tag{38}$$

$$z_5 = 2B + 4B_4x^2 + \ldots, \tag{39}$$

where $B_4, B_6, \ldots, \gamma_2, \gamma_4, \ldots, A_3, A_5, \ldots$ involve only A and B. A five-point finite difference formula (Fox 1957) was substituted for the derivatives in (30)–(34), arbitrary values of A and B were assigned, and (30)–(34) were integrated step-by-step for intervals of $\Delta x = 0{\cdot}01$. (The first four values of z_i and $\dot{z}_i$ were obtained from the Taylor series (35)–(39).) At each step, a computation was made of

$$\alpha_n \equiv z_2 - \frac{z_1^2}{4x^2}.$$

This quantity tends to a constant at large x. When $|\alpha_{n+1} - \alpha_n|$ fell below 10^{-6}, the forward integration was stopped and the last $\alpha_n (\equiv \delta)$ was recorded. *Holding B fixed*, A was varied, a new integration was performed and a new δ obtained. A linear extrapolation was then made using the two A's and the two associated values of δ to form an estimate of A corresponding to $\delta = 0$. The procedure was

continued until an A was obtained with an associated δ of absolute value below 10^{-3}. Over the entire range of the integration it was only necessary to integrate forward to values of x of 4 or 5.

The final pair (A, B) obtained in this manner corresponds to a solution of the problem if, according to (25), we take the resulting asymptotic value of z_1 to be $c^{-\frac{1}{4}}$, since then we have $\Gamma \to 1$ and $s \to 0$. When, at any stage, a final pair (A, B) was obtained with the desired $|\delta| \leqslant 10^{-3}$, the search for the next pair, corresponding to a new value of B, was begun by using the two new trial pairs $(A, B \mp 0{\cdot}02)$,

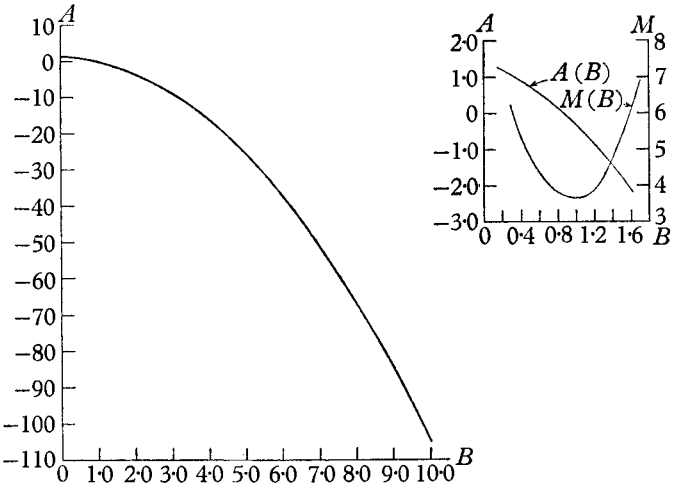

FIGURE 2. Plots of curves $A = A(B)$ and $M = M(B)$.

$(A \pm 0{\cdot}02, B \mp 0{\cdot}02)$ depending on whether the march along the curve $A = A(B)$ in the A–B plane was toward lower B or higher B. This procedure was suggested by a few hand integrations which indicated that the curve $A = A(B)$ has a slope of the order of -1. (Actually the curve has a slope of approximately $-2B$ throughout the range.) The interval in B was increased to 0·04 and 0·05 for large B. Finally, it should be mentioned that the search for the curve $A = A(B)$ was begun by using two initial pairs for (A, B): (0·497, 0·660) and (0·510, 0·660). The hand integrations showed that the curve $A = A(B)$ lies in the vicinity of these two points.

4. Results of numerical integration

A large number of numerical solutions were obtained at intervals of 0·02 or 0·04 or 0·05 in B over the range† $0{\cdot}18 \leqslant B \leqslant 10{\cdot}02$. Figure 2 is a plot of the two curves $A = A(B)$ and $M = M(B)$, and table 1 is a list of the triples of numbers $(A, B, c^{-\frac{1}{4}})$. As mentioned above, A decreases regularly as B increases. A surprising result is that the non-dimensional momentum transfer does not uniquely determine the flow; above a minimum M there are two solutions for each M.

† If the pair (A, B) yields a solution, $(A, -B)$ is a solution with the same velocity and pressure fields except for a reverse circulating motion. This is easily seen from the form of the Taylor series expansion. The convergence of the present method of finding solutions became slower and slower near $B = 0$, and it was necessary to stop at $B = 0{\cdot}18$.

Since $M = J/K^2$, where J is the kinematic momentum transfer, J must be positive and larger than a critical value $J_0 = 3{\cdot}65K^2$.

The velocity and pressure profiles are given in a series of figures. In figures 3–9, we see that the axial velocity at the axis is away from the point of singularity in

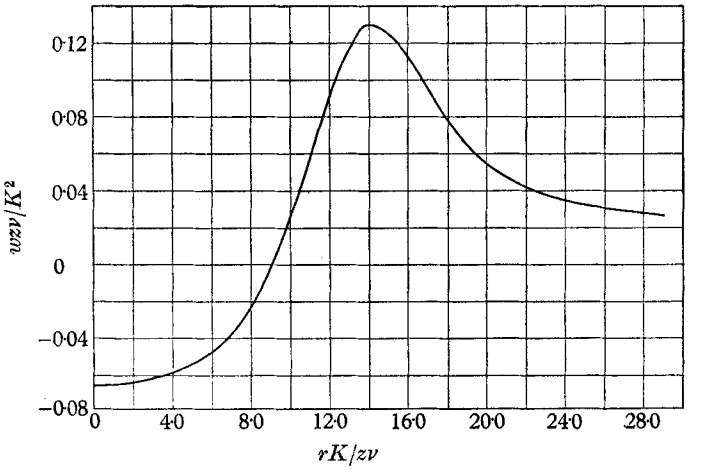

FIGURE 3. w-curve: $B = 0{\cdot}180$.

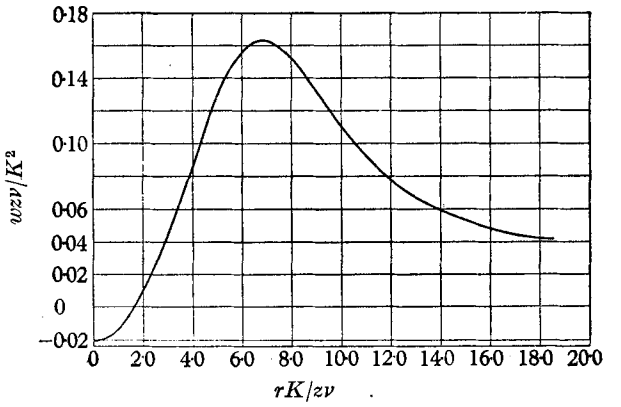

FIGURE 4. w-curve: $B = 0{\cdot}800$.

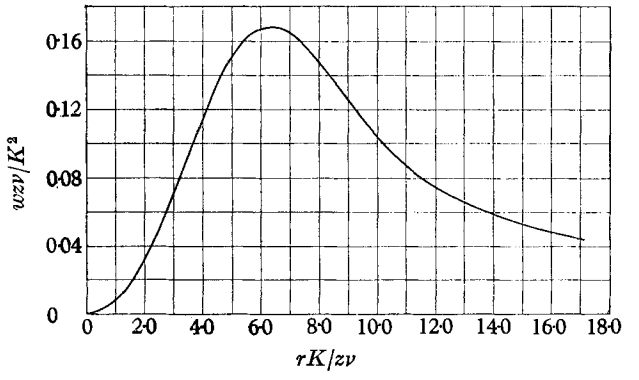

FIGURE 5. w-curve for $A = 0$ (vortex with a thin wire in the core).

most of the solutions. There is a solution (figure 5), however, in which the axial velocity at the axis of the core is precisely zero, and there is a range ($A > 0$) in which the velocity is toward the singularity. As A decreases from zero to $-\sqrt{2}$ there is a deficiency of velocity at the axis. This is finally wiped out for $A < -\sqrt{2}$ and for larger A there is simply a thin upward jet in the vortex core.

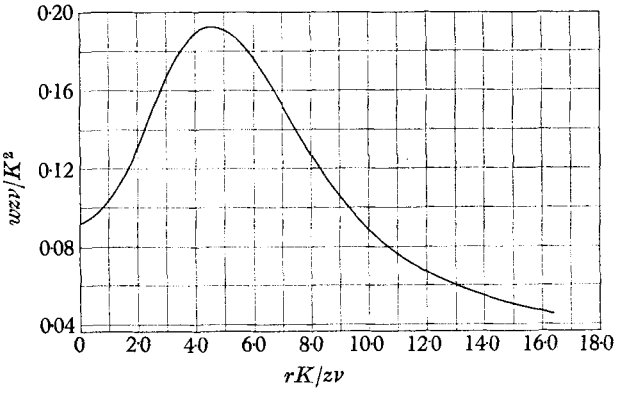

FIGURE 6. w-curve: $B = 1{\cdot}10$.

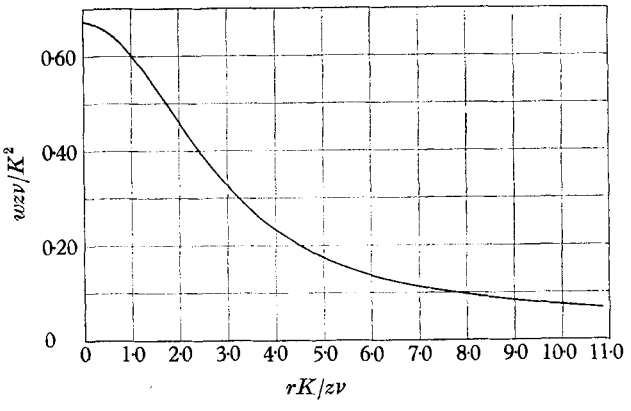

FIGURE 7. w-curve: $B = 1{\cdot}70$.

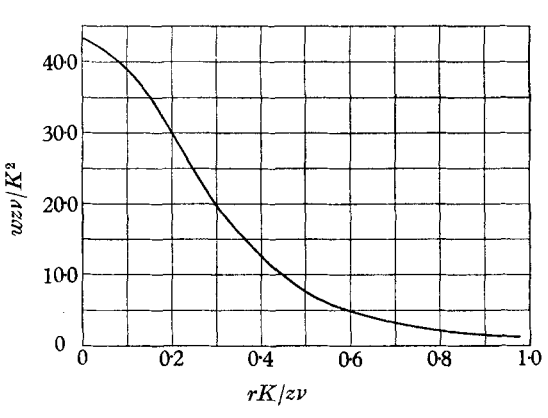

FIGURE 8. w-curve: $B = 5{\cdot}02$.

These features of the axial velocity profile are understandable from the viewpoint of energy variation. Thus, it is easily shown that if E is the total of pressure energy and kinetic energy, the energy variation following particles moving along the axis is

$$\frac{dE}{dt} = \frac{2K^6c^{\frac{3}{2}}A}{\nu^3 z^4}\left(\frac{A^2}{2} - 1\right).$$

For example, when the velocity is away from the singularity ($A < 0$) and in the range $A^2 < 2$, the particle gains energy from its surroundings, as the faster moving fluid just out from the axis exerts a drag in the direction of the flow. When ($0 < A < \sqrt{2}$) the fluid moving toward the singularity is imbedded in fluid moving the other way. The result is a loss of energy to the surroundings. Trial integrations for $A > \sqrt{2}$ suggested that there is no branch of the $A = A(B)$ curve for this range of A.

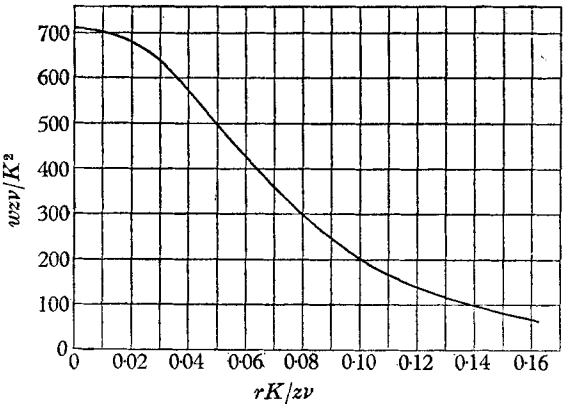

FIGURE 9. w-curve: $B = 10{\cdot}02$.

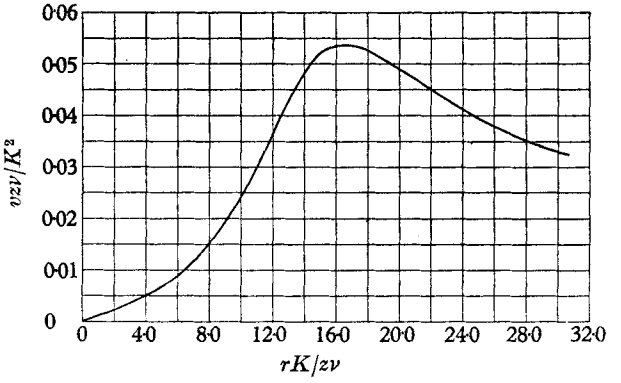

FIGURE 10. v-curve: $B = 0{\cdot}180$.

The theoretical behaviour of the axial velocity far from the axis is $w \to K/r\sqrt{2}$, and this was verified by all the numerical integrations.

The circulating velocity curves (figures 10–13) are all similar. We see, however, in figure 13, that as B tends to infinity the swirling motion approaches solid rotation in the core, changing more and more abruptly to a vr-vortex outside. In all cases, of course, $v \to K/r$ as $r \to \infty$.

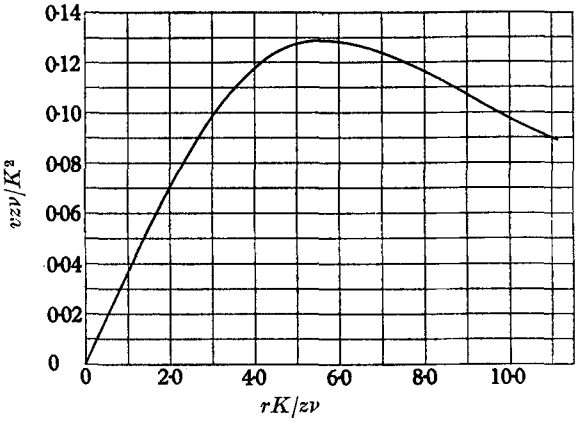

FIGURE 11. v-curve: $B = 1{\cdot}10$.

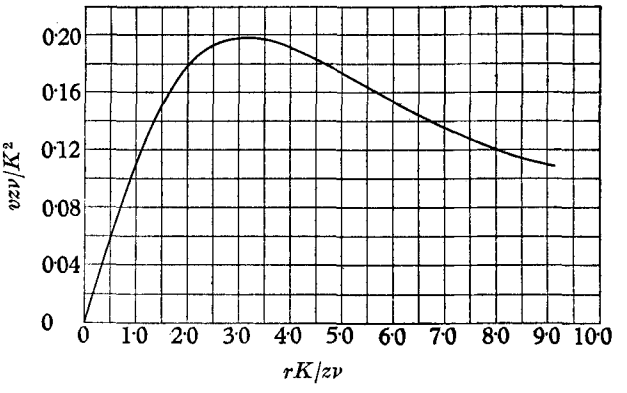

FIGURE 12. v-curve: $B = 1{\cdot}70$.

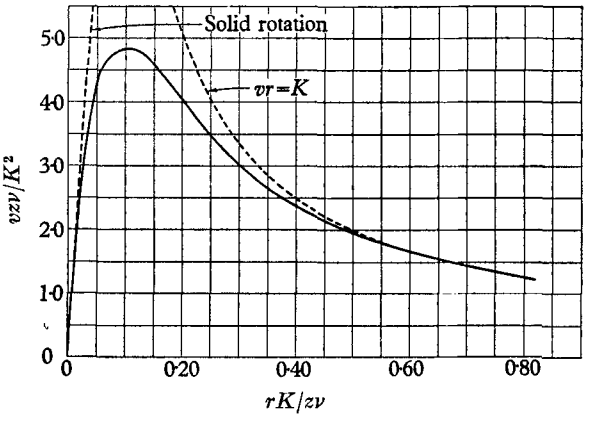

FIGURE 13. v-curve: $B = 10{\cdot}02$.

The outward-motion curves or u-curves (figures 14–17) have two characteristic shapes. In all cases there is inward motion at the outer edges of the vortex, as indicated by the theoretical behaviour $u \to -\nu/r$, and outward motion in most of the vortex core. In some cases, however, as in figures 14 and 15, inward motion

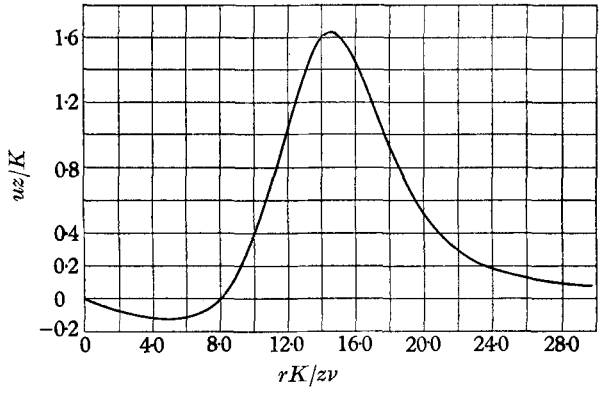

FIGURE 14. u-curve: $B = 0{\cdot}180$.

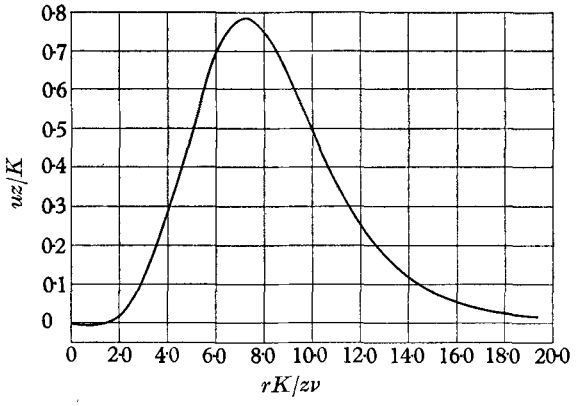

FIGURE 15. u-curve: $B = 0{\cdot}800$.

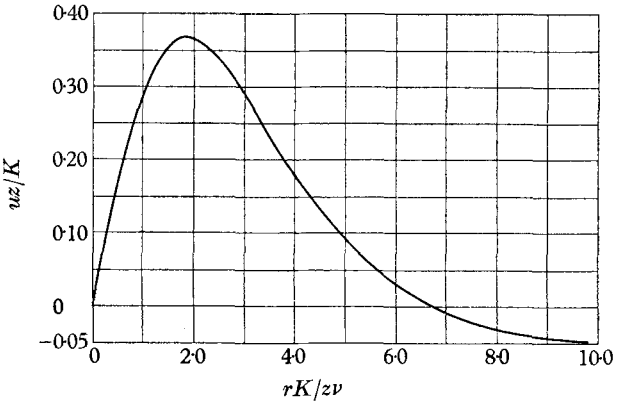

FIGURE 16. u-curve: $B = 1{\cdot}70$.

can occur near the axis. It is important to notice, of course, that v and w are large and of the same order ($\sim K/r$) while u is extremely small in a well-developed vortex.

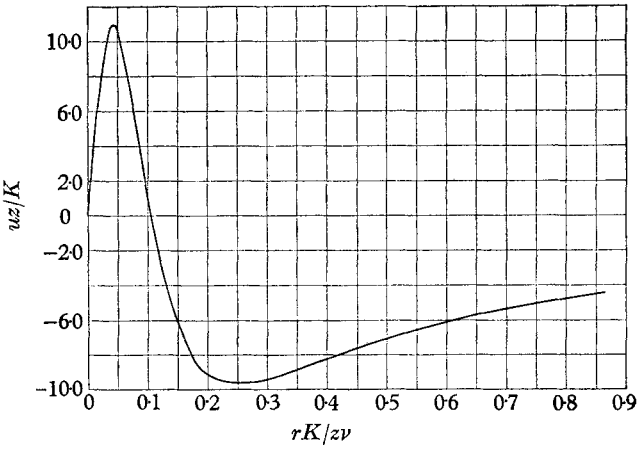

FIGURE 17. u-curve: $B = 10{\cdot}02$.

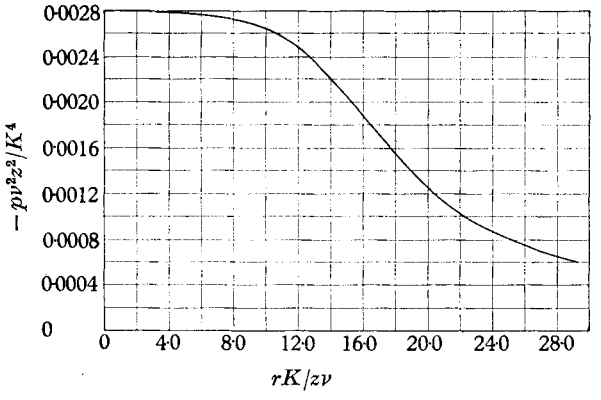

FIGURE 18. p-curve: $B = 0{\cdot}180$.

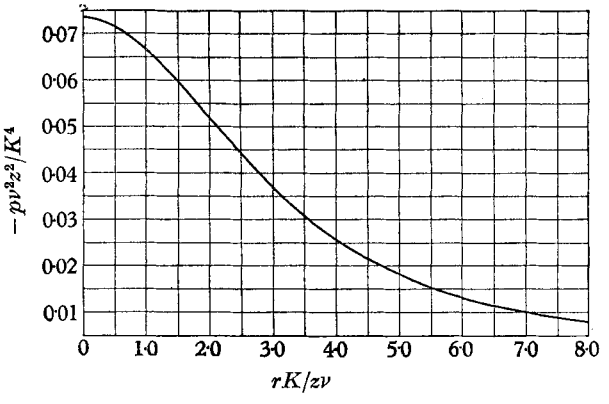

FIGURE 19. p-curve: $B = 1{\cdot}70$.

The pressure is determined completely by the centrifugal force in the boundary-layer approximation, so that it drops monotonically from zero outside to a negative minimum at the axis, as shown in figures 18 and 19.

The radius of the vortex boundary layer, δ, is an interesting feature of the solution. Over the entire range of the numerical integrations, the value of x at, say, maximum v, decreases only by a factor of 2 or so. If we neglect this variation we can write $\delta \sim (z\nu/K)\, c^{-\frac{1}{4}}$.

5. Vortices in confined fluids

Intense vortices occur frequently in fluids. One kind is the 'bathtub drain' vortex which is characterized by the presence of a free surface, and is probably not related closely, if at all, to the vortex of this paper. Another is the vortex without free surface which has a rigid boundary like the bottom of the vessel in

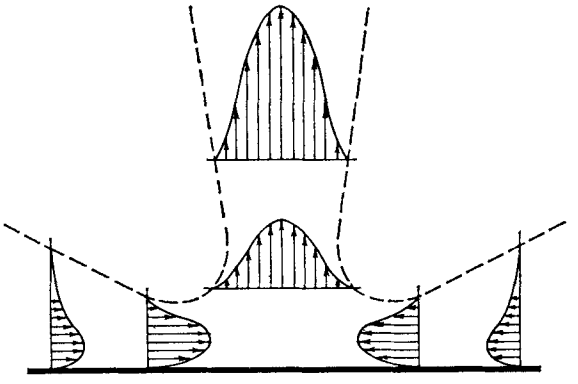

FIGURE 20. Schematic picture of plate boundary layer.

the experiment of figure 1. The latter may be closely related to the meteorological vortices, tornadoes, dust whirls and water spouts (if we adopt the virtual viscosity concept), although the atmospheric vortices are probably 'buoyancy driven' rather than 'momentum driven'. It seems very likely that tornadoes, for example, are *vr*-vortices. We have at least one very reliable set of observations that indicates this, namely eight pressure observations in the outskirts of a tornado that passed through an NACA laboratory in Cleveland, Ohio (Lewis & Perkins 1953). They yielded the precise pressure distribution of a *vr*-vortex if we assume a balance of centrifugal and pressure gradient forces as in the vortex of this paper. The pressure observations were at the ground, and if we assume that they reflect the velocity of circulation in the free air, rather than in the ground boundary layer (as supposed by Lewis & Perkins) we obtain a reliable estimate of K of $7{\cdot}5 \times 10^7$ cm^2/sec.

We can imagine a schematic picture of flow from the plate or ground boundary layer in the experimental and geophysical vortices as in figure 20, and it is tempting to try to fit one of the theoretical vortices of this paper ($A < -\sqrt{2}$) to this flow with a virtual source at some great distance *below* the plate. One would have to suppose that the velocity distribution as the fluid leaves the plate is nearly the same as in the infinite vortex at some definite section.

In fact this is far from the truth in the experiment. Measurements show, for example, that w drops off much faster than $K/r\sqrt{2}$ at the outer edge of the core. We cannot hope, therefore, to get agreement between experiment and theory unless we compare them at such a great distance from the plate that the slight viscous effect will have enough time to cause a change of velocity distribution from that which the fluid has when it leaves the plate boundary layer to that which it has in the infinite vortex. A plausible estimate of this distance Δz can be obtained by assuming that the theoretical vortex of this paper must suffer a change of radius $\Delta\delta$ over this distance of the same order as the radius δ itself just above the plate. Thus, from (6), we have $\Delta z/\Delta\delta \sim 1/\epsilon c^{-\frac{1}{4}}$, and, putting $\Delta\delta/\delta \sim 1$, we get $\Delta z \sim \delta/\epsilon c^{-\frac{1}{4}}$. Since $c^{-\frac{1}{4}} \sim 1$ and, in the experiment, $\delta \sim 1$ cm, $\epsilon \sim 10^{-3}$, we would need a height $\Delta z \sim 10^3$ cm before we could expect any significant effect of viscosity transforming the vortex into one resembling the theoretical vortex of this paper. A similar calculation for a tornado yields 10^6 cm, or about the depth of the troposphere, if we take $\epsilon = 10^{-2}$. The above reasoning indicates that the experimental vortex as observed in the laboratory is not a member of the family of vortices of this paper, and a separate theory is necessary to discuss its features. This may also be true of atmospheric vortices, at least near the ground.

The research was supported by the Office of Naval Research and the U.S. Weather Bureau. The author wishes to thank Dr Joseph Smagorinsky for his help in the computational work of the paper.

REFERENCES

Fox, L. 1957 *Two-point Boundary Problems.* Oxford University Press.

Lewis, W. & Perkins, P. J. 1953 Recorded pressure distribution in the outer portion of a tornado vortex. *Monthly Weather Review*, **81**, 379.

Long, R. R. 1958. Vortex motion in a viscous fluid. *J. Meteor.* **15**, 108.

Long, R. R. 1956 Sources and sink at the axis of a rotating liquid. *Quart. J. Mech. Appl. Math.* **9**, 385.

A	B	$c^{-\frac{1}{2}}$	A	B	$c^{-\frac{1}{2}}$	A	B	$c^{-\frac{1}{2}}$	A	B	$c^{-\frac{1}{2}}$	A	B	$c^{-\frac{1}{2}}$
1·26	0·160	4·45	−0·838	1·20	2·36	− 6·89	2·66	1·37	−24·5	4·92	0·786	− 58·2	7·52	0·515
1·24	0·180	4·35	−0·896	1·22	2·34	− 7·11	2·70	1·36	−25·0	4·97	0·778	− 59·0	7·57	0·511
1·21	0·200	4·26	−0·953	1·24	2·32	− 7·33	2·74	1·34	−25·5	5·02	0·771	− 59·8	7·62	0·508
1·19	0·220	4·18	−1·01	1·26	2·30	− 7·56	2·78	1·32	−26·0	5·07	0·763	− 60·6	7·67	0·504
1·16	0·240	4·11	−1·07	1·28	2·28	− 7·79	2·82	1·31	−26·6	5·12	0·756	− 61·4	7·72	0·501
1·13	0·260	4·04	−1·13	1·30	2·26	− 8·03	2·86	1·29	−27·1	5·17	0·749	− 62·2	7·77	0·498
1·11	0·280	3·97	−1·19	1·32	2·24	− 8·26	2·90	1·28	−27·6	5·22	0·742	− 63·1	7·82	0·495
1·08	0·300	3·90	−1·25	1·34	2·22	− 8·51	2·94	1·26	−28·2	5·27	0·735	− 63·9	7·87	0·491
1·05	0·320	3·84	−1·32	1·36	2·20	− 8·75	2·98	1·25	−28·7	5·32	0·728	− 64·7	7·92	0·488
1·02	0·340	3·78	−1·38	1·38	2·18	− 9·00	3·02	1·23	−29·3	5·37	0·721	− 65·5	7·97	0·485
0·991	0·360	3·73	−1·41	1·39	2·17	− 9·25	3·06	1·22	−29·8	5·42	0·715	− 66·4	8·02	0·482
0·960	0·380	3·68	−1·44	1·40	2·16	− 9·50	3·10	1·21	−30·4	5·47	0·708	− 67·2	8·07	0·479
0·929	0·400	3·62	−1·47	1·41	2·15	− 9·76	3·14	1·19	−31·0	5·52	0·702	− 68·1	8·12	0·476
0·897	0·420	3·57	−1·51	1·42	2·15	−10·0	3·18	1·18	−31·5	5·57	0·696	− 69·0	8·17	0·473
0·864	0·440	3·53	−1·54	1·43	2·14	−10·3	3·22	1·17	−32·1	5·62	0·690	− 69·9	8·22	0·470
0·831	0·460	3·48	−1·57	1·44	2·13	−10·6	3·26	1·15	−32·7	5·67	0·684	− 70·7	8·27	0·467
0·797	0·480	3·44	−1·60	1·45	2·12	−10·8	3·30	1·14	−33·3	5·72	0·678	− 71·6	8·32	0·464
0·763	0·500	3·39	−1·64	1·46	2·11	−11·1	3·34	1·13	−33·9	5·77	0·672	− 72·5	8·37	0·461
0·728	0·520	3·35	−1·67	1·47	2·10	−11·4	3·38	1·12	−34·5	5·82	0·666	− 73·4	8·42	0·459
0·692	0·540	3·31	−1·70	1·48	2·09	−11·6	3·42	1·11	−35·1	5·87	0·660	− 74·3	8·47	0·456
0·656	0·560	3·27	−1·73	1·49	2·08	−11·9	3·46	1·09	−35·7	5·92	0·655	− 75·2	8·52	0·453
0·619	0·580	3·23	−1·77	1·50	2·08	−12·2	3·50	1·08	−36·3	5·97	0·649	− 76·1	8·57	0·450
0·581	0·600	3·19	−1·84	1·52	2·07	−12·5	3·54	1·07	−37·0	6·02	0·644	− 77·0	8·62	0·448
0·543	0·620	3·16	−1·90	1·54	2·04	−12·8	3·58	1·06	−37·6	6·07	0·639	− 77·9	8·67	0·445
0·504	0·640	3·12	−1·97	1·56	2·02	−13·1	3·62	1·05	−38·2	6·12	0·634	− 78·9	8·72	0·442
0·465	0·660	3·08	−2·04	1·58	2·01	−13·4	3·66	1·04	−38·9	6·17	0·628	− 79·8	8·77	0·440
0·425	0·680	3·05	−2·18	1·62	1·98	−13·7	3·70	1·03	−39·5	6·22	0·623	− 80·7	8·82	0·437
0·384	0·700	3·02	−2·33	1·66	1·95	−14·0	3·74	1·02	−40·2	6·27	0·618	− 81·7	8·87	0·435
0·343	0·720	2·98	−2·47	1·70	1·92	−14·3	3·78	1·01	−40·8	6·32	0·613	− 82·6	8·92	0·432
0·301	0·740	2·95	−2·62	1·74	1·89	−14·6	3·82	1·00	−41·5	6·37	0·609	− 83·6	8·97	0·430
0·258	0·760	2·92	−2·78	1·78	1·87	−14·9	3·86	0·990	−42·1	6·42	0·604	− 84·5	9·02	0·427
0·215	0·780	2·89	−2·93	1·82	1·83	−15·2	3·90	0·981	−42·8	6·47	0·599	− 85·5	9·07	0·425
1·171	0·800	2·86	−3·09	1·86	1·80	−15·6	3·94	0·971	−43·5	6·52	0·595	− 86·5	9·12	0·422
0·126	0·820	2·83	−3·25	1·90	1·76	−15·9	3·98	0·962	−44·2	6·57	0·590	− 87·5	9·17	0·420
0·082	0·840	2·80	−3·42	1·94	1·75	−16·2	4·02	0·953	−44·9	6·62	0·586	− 88·5	9·22	0·418
0·036	0·860	2·77	−3·58	1·98	1·72	−16·6	4·07	0·942	−45·6	6·67	0·581	− 89·4	9·27	0·415
−0·010	0·880	2·75	−3·75	2·02	1·70	−17·1	4·12	0·931	−46·3	6·72	0·577	− 90·4	9·32	0·413
−0·057	0·900	2·72	−3·93	2·06	1·68	−17·5	4·17	0·921	−47·0	6·77	0·572	− 91·4	9·37	0·411
−0·105	0·920	2·69	−4·10	2·10	1·65	−17·9	4·22	0·911	−47·7	6·82	0·568	− 92·4	9·42	0·409
−0·153	0·940	2·66	−4·28	2·14	1·63	−18·4	4·27	0·900	−48·4	6·87	0·564	− 93·5	9·47	0·406
−0·202	0·960	2·64	−4·46	2·18	1·61	−18·8	4·32	0·891	−49·1	6·92	0·560	− 94·5	9·52	0·404
−0·251	0·980	2·61	−4·65	2·22	1·58	−19·2	4·37	0·881	−49·8	6·97	0·556	− 95·5	9·57	0·402
−0·301	1·00	2·59	−4·84	2·26	1·56	−19·7	4·42	0·871	−50·6	7·02	0·552	− 96·5	9·62	0·400
−0·352	1·02	2·56	−5·03	2·30	1·54	−20·1	4·47	0·862	−51·3	7·07	0·548	− 97·6	9·67	0·398
−0·403	1·04	2·54	−5·22	2·34	1·52	−20·6	4·52	0·853	−52·1	7·12	0·544	− 98·6	9·72	0·396
−0·456	1·06	2·52	−5·42	2·38	1·50	−21·1	4·57	0·844	−52·8	7·17	0·540	− 99·7	9·77	0·394
−0·508	1·08	2·49	−5·62	2·42	1·48	−21·6	4·62	0·835	−53·6	7·22	0·536	−100·7	9·82	0·392
−0·562	1·10	2·47	−5·82	2·46	1·46	−22·0	4·67	0·827	−54·3	7·27	0·533	−101·8	9·87	0·390
−0·616	1·12	2·45	−6·03	2·50	1·44	−22·5	4·72	0·818	−55·1	7·32	0·529	−102·8	9·92	0·388
−0·670	1·14	2·42	−6·24	2·54	1·43	−23·0	4·77	0·810	−55·9	7·37	0·525	−103·9	9·97	0·385
−0·726	1·16	2·40	−6·45	2·58	1·41	−23·5	4·82	0·802	−56·6	7·42	0·522	−105·0	10·02	0·383
−0·782	1·18	2·38	−6·67	2·62	1·39	−24·0	4·87	0·794	−57·4	7·47	0·518	—	—	—

TABLE 1. List of triples (A, B, $c^{-\frac{1}{2}}$) yielded by numerical integration.

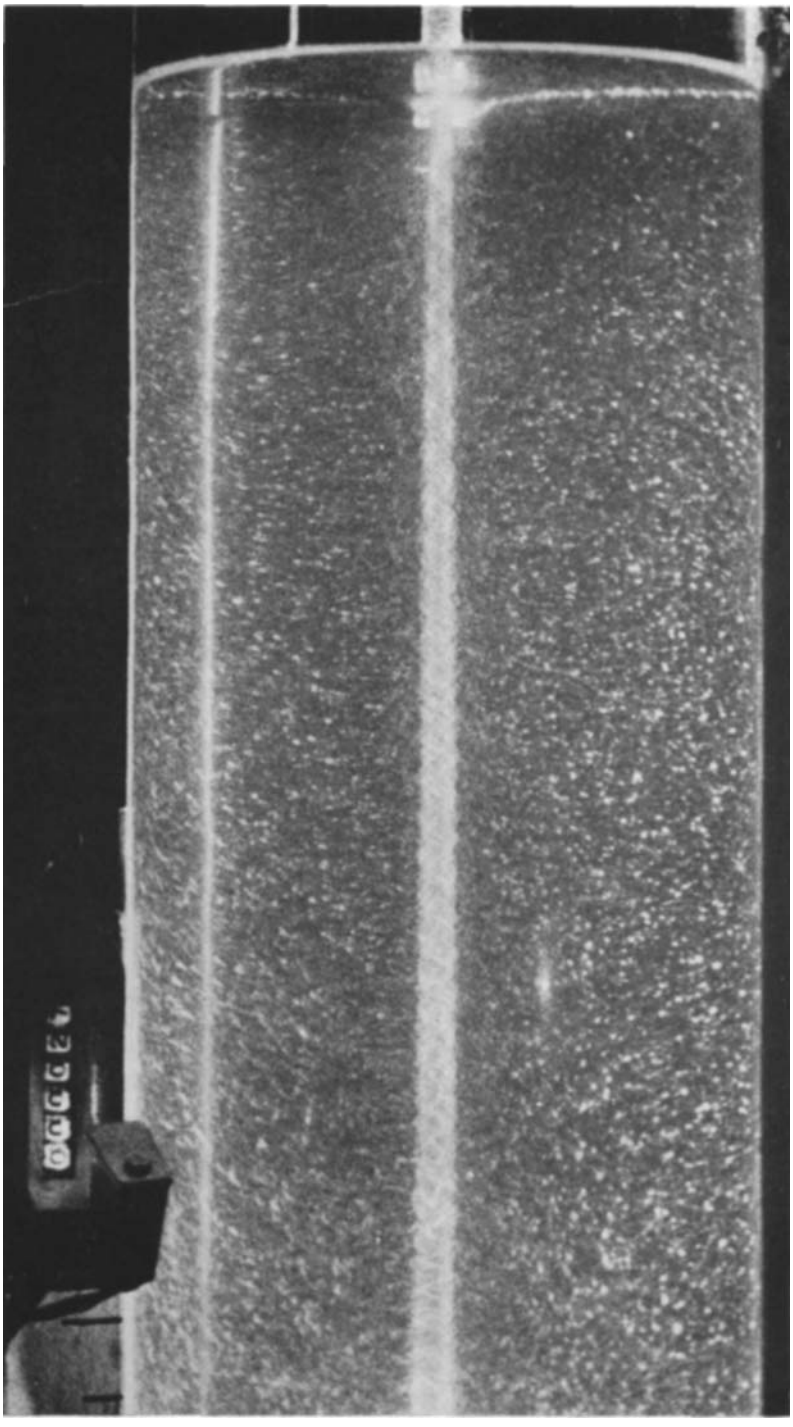

FIGURE 1 (PLATE 1). Experimental vortex. This vortex is created by withdrawing water from the axis of a rotating vessel 1 m high and 30 cm in diameter. The sink is just below the free surface at the top of the figure. The motion near the axis is one of strong rotation superimposed on a strong motion toward the sink. This is indicated by the spiral nature of the streaks on the $\frac{1}{5}$-second time-exposure caused by the aluminum tristearate tracer. The vortex extends to the bottom of the vessel where there is a layer of particles. This explains the dense collection of particles near the axis.